

# UC Berkeley

## UC Berkeley Previously Published Works

### Title

In Situ Potentiodynamic Analysis of the Electrolyte/Silicon Electrodes Interface Reactions - A Sum Frequency Generation Vibrational Spectroscopy Study

### Permalink

<https://escholarship.org/uc/item/0qd4f09v>

### Journal

Journal of the American Chemical Society, 138(3)

### ISSN

0002-7863

### Authors

Horowitz, Yonatan  
Han, Hui-Ling  
Ross, Philip N  
[et al.](#)

### Publication Date

2016-01-27

### DOI

10.1021/jacs.5b10333


Peer reviewed

## 1 In Situ Potentiodynamic Analysis of the Electrolyte/Silicon Electrodes 2 Interface Reactions - A Sum Frequency Generation Vibrational 3 Spectroscopy Study

4 Yonatan Horowitz,<sup>§,†,‡</sup> Hui-Ling Han,<sup>§,†</sup> Philip N. Ross,<sup>†</sup> and Gabor A. Somorjai<sup>\*,†,‡</sup>

5 <sup>†</sup>Materials Sciences Division, Lawrence Berkeley National Laboratory, 1 Cyclotron Road, Berkeley, California 94720, United States

6 <sup>‡</sup>Department of Chemistry, University of California, Berkeley, California 94720, United States

7  Supporting Information

8 **ABSTRACT:** The key factor in long-term use of batteries  
9 is the formation of an electrically insulating solid layer that  
10 allows lithium ion transport but stops further electrolyte  
11 redox reactions on the electrode surface, hence solid  
12 electrolyte interphase (SEI). We have studied a common  
13 electrolyte, 1.0 M LiPF<sub>6</sub>/ethylene carbonate (EC)/diethyl  
14 carbonate (DEC), reduction products on crystalline silicon  
15 (Si) electrodes in a lithium (Li) half-cell system under  
16 reaction conditions. We employed in situ sum frequency  
17 generation vibrational spectroscopy (SFG-VS) with inter-  
18 face sensitivity in order to probe the molecular  
19 composition of the SEI surface species under various  
20 applied potentials where electrolyte reduction is expected.  
21 We found that, with a Si(100)-hydrogen terminated wafer,  
22 a Si-ethoxy (Si-OC<sub>2</sub>H<sub>5</sub>) surface intermediate forms due to  
23 DEC decomposition. Our results suggest that the SEI  
24 surface composition varies depending on the termination  
25 of Si surface, i.e., the acidity of the Si surface. We provide  
26 the evidence of specific chemical composition of the SEI  
27 on the anode surface under reaction conditions. This  
28 supports an electrochemical electrolyte reduction mecha-  
29 nism in which the reduction of the DEC molecule to an  
30 ethoxy moiety plays a key role. These findings shed new  
31 light on the formation mechanism of SEI on Si anodes in  
32 particular and on SEI formation in general.

33 **L**ithium ion batteries are one of the most common forms of  
34 energy storage devices.<sup>1,2</sup> For electric vehicles where  
35 higher capacity is needed, the silicon based anodes are attractive  
36 candidates to replace graphite based anodes due to its  
37 theoretical capacity<sup>3</sup> of 4008 mAh/g. However, the Si lattice  
38 expands up to four times its volume,<sup>4</sup> which results in  
39 irreversible capacity loss and short cycling lifetime due to  
40 continued cracking and electrolyte consumption on the  
41 exposed Si surface.<sup>5</sup> The key factor in long-term use (cyclability  
42 and stability) of such devices is the formation of an electrically  
43 insulating layer that allows lithium ion transport at a reasonable  
44 rate while hindering electrolyte consumption on the Si anode  
45 surface, and is termed the solid electrolyte interphase (SEI).<sup>5-7</sup>  
46 Previous studies from this laboratory have indicated that the  
47 nature of the electrolyte consuming reactions in lithium  
48 batteries is electrode material dependent.<sup>8,9</sup>

Specifically, a study using ex situ infrared vibrational 49  
spectroscopy observed two different SEI compositions on Sn 50  
and Ni electrodes<sup>10</sup> even though the same electrolyte solution 51  
was used. Therefore, we may expect the electrolyte consuming 52  
reactions on Si may be unique to this surface and that the 53  
nature of the reactions may be a critical factor in determining 54  
the functioning of the surface layer formed, i.e. whether it 55  
functions as an SEI. The successful replacement of graphite by 56  
Si may require a detailed understanding of these surface<sup>11</sup>  
reactions and the ability to manipulate them by surface<sup>12-14</sup> or 57  
electrolyte modification<sup>15</sup> in particular by adding fluorinated 58  
EC to the electrolyte solution.<sup>16,17</sup> 60

A major obstacle in determining the SEI formation and 61  
composition is the practice of ex situ, post-cycling examination 62  
of lithiated samples that inevitably leads to loss of information. 63  
The need for a surface-sensitive technique that enables 64  
nondestructive and in situ analysis of the SEI chemistry such 65  
as SFG-VS<sup>18</sup> is crucial. SFG-VS was used successfully in 66  
previous electrochemical systems<sup>19</sup> on metallic electrodes 67  
(copper, gold)<sup>20,21</sup> as well as on cathode oxide materials 68  
(LiCoO<sub>2</sub>).<sup>22,23</sup> We present the SFG-VS spectra of surface- 69  
electrochemical reactions in situ on a silicon anode and the 70  
differences between an oxide termination (SiO<sub>2</sub>) and hydrogen 71  
one (Si-H).<sup>24</sup> We took the SFG-VS spectra under working 72  
conditions at three potential ranges. The voltogram shown in 73  
Figure 1 was taken with a Si(100)-hydrogen terminated surface 74  
and has three reduction peaks at ~1.5, ~0.5, and ~0.10 V that 75  
are consistent with values reported in the literature.<sup>25</sup> 76

Therefore, we divide the potential range into three narrower 77  
ones. The first potential range (referred as ~1 V) is at 1.1 to 0.8 78  
V versus Li/Li<sup>+</sup> since no major reduction of EC molecules is 79  
expected. The second potential ranges between 0.65 V and 0.35 80  
V (referred as ~0.5 V) since EC molecules undergo several 81  
reduction reactions at this potential range. The third potential 82  
range was chosen between -0.05 to 0.10 V where lithiation is 83  
expected (referred as ~0.1 V). 84

In Figure 2a, for the Si(100)-H electrode, we show the 85  
divided SFG spectrum after applying a 30 cycle cyclic- 86  
voltammetry (CV) potential near 1 V by the SFG in open 87  
circuit potential (OCP). Dividing the SFG spectra emphasizes 88  
the appearance of ethoxy group vibrational peaks (black line). 89  
The SFG from the Si/SEI is interfered with by the SFG 90

Received: October 5, 2015

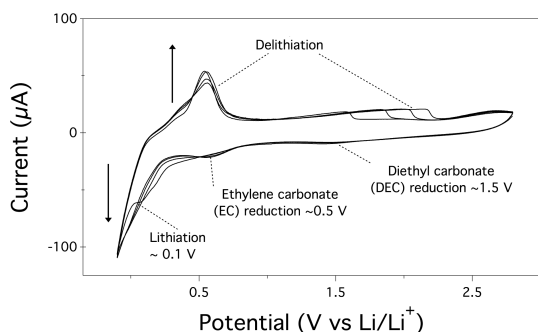


**Figure 1.** Three reduction peaks at a Si(100)-H anode of the electrolyte (1.0 M LiPF<sub>6</sub> in EC: DEC, 1:2 v/v) are presented in this CV plot. The reduction of DEC is around 1.5 V. The reduction of EC is about 0.5 V, and Li intercalation (lithiation) occurs around 0.10 V. Scan rate was 1 mV/s.

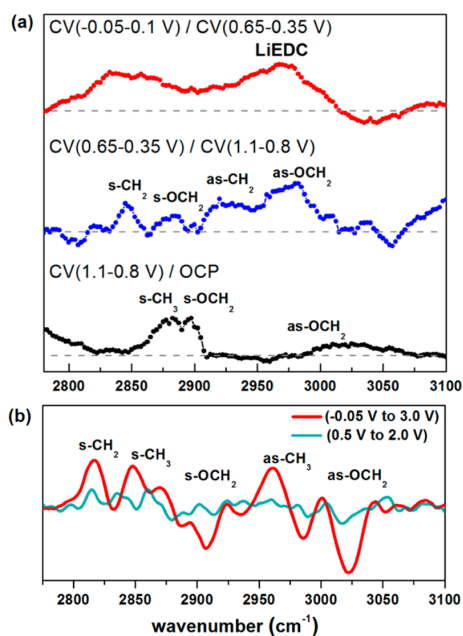


**Figure 2.** (a) We show the evolution of SFG signal under reaction conditions of crystalline silicon Si(100)-hydrogen terminated anode. The SFG spectra were taken at open circuit potential and after cyclic voltammetry at 1.1 V ↔ 0.8 V, 0.65 V ↔ 0.35 V, and 0.1 V ↔ -0.05 V. In order to emphasize the evolution of the Si-ethoxy peaks we divided the SFG spectra by their former potentials, as follows: SFG<sub>1.1 V ↔ 0.8 V</sub>/OCP (black), SFG<sub>0.65 V ↔ 0.35 V</sub>/SFG<sub>1.1 V ↔ 0.8 V</sub> (blue), and SFG<sub>-0.05 V ↔ 0.1 V</sub>/SFG<sub>0.65 V ↔ 0.35 V</sub> (red). (b) The SFG profiles of crystalline silicon oxide Si(100) anode after cycling between 0.5 V ↔ 2.0 V (blue) and -0.05 V ↔ 3.0 V (red). All CVs were repeated for 30 cycles at a scan rate of 1 mV/s.

91 generated from the Si substrate.<sup>26</sup> We assume that if an  
92 intermediate species ethoxy radical<sup>27,28</sup> •OCH<sub>2</sub>CH<sub>3</sub> (or anion,  
93 <sup>-</sup>OCH<sub>2</sub>CH<sub>3</sub>)<sup>29</sup> is formed near the Si anode surface, it will react  
94 with Si-H to produce a Si-OCH<sub>2</sub>CH<sub>3</sub> bond. This reaction  
95 cannot take place if a thick passivating oxide layer is present. In  
96 Figure 2a, we assigned the SFG peaks corresponding to Si-  
97 ethoxy bonds according to the work by Bateman et al.,<sup>30</sup> and  
98 SFG peaks relating to the various SEI components are as

follows:<sup>31,32</sup> 2875 cm<sup>-1</sup> (s-CH<sub>3</sub>), 2895 cm<sup>-1</sup> (s-OCH<sub>2</sub>), and  
2975 and 3025 cm<sup>-1</sup> (both as-OCH<sub>2</sub>).

After a 30 cycle CV at ~0.5 V (blue line), we observed peaks  
appearing at 2845 cm<sup>-1</sup> (s-CH<sub>2</sub>), 2895 cm<sup>-1</sup> (s-OCH<sub>2</sub>), 2920  
cm<sup>-1</sup> (as-CH<sub>2</sub>), and 2975 and 3025 cm<sup>-1</sup> (as-OCH<sub>2</sub>). Most  
hydrocarbon molecules cannot be identified conclusively  
without using the whole IR spectrum. For example, poly-EC  
cannot be identified as such without using the asymmetric C-  
O-C band around 1100 cm<sup>-1</sup> that is unique to poly-EC vs  
either DEC or EC. Therefore, we can only suggest our  
interpretation to the assigned products. Nevertheless, we  
attribute these observations to the EC molecules undergoing  
a reduction reaction into poly-EC and other ethyl carbonate  
species, as well as interact with DEC moieties. These reduction  
reactions are attributed to the beginning of the SEI  
formation.<sup>33-35</sup>

The SFG spectra taken after 30 CV between 0.1 V and -0.05  
V (red line) show increasing peaks at 2850 cm<sup>-1</sup>, and 2960  
cm<sup>-1</sup>, presumably due to the formation of lithium ethylene  
dicarbonate (LiEDC) and poly-EC. The peaks broaden due to  
surface deterioration after lithiation.

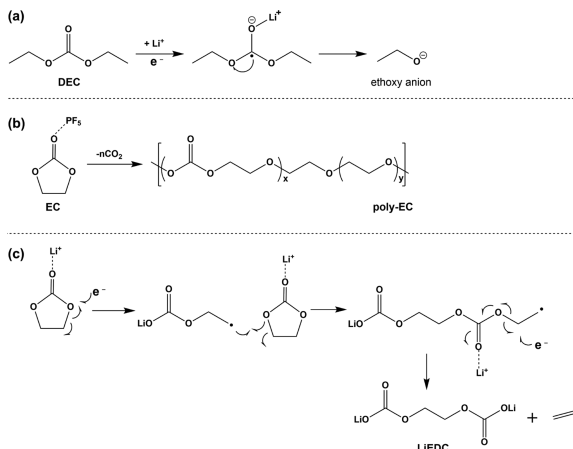
In the case of Si(100) oxide we did not observe any change  
at ~1 V; therefore, we extended the CV potential range. In  
Figure 2b, we compare the SFG spectra of the crystalline  
Si(100) oxide surface before and after lithiation. We performed  
a potential sweep in the range of 0.5 V to 2.0 V (blue profile)  
and between -0.05 V and 3.0 V. Each CV had 30 cycles, and  
the rate was 1 mV/s. The SFG profile of the first potential  
range (blue) has some SEI features but none that are related to  
a Si-O to Si-OC<sub>2</sub>H<sub>5</sub> substitution reaction. After lithiation  
(red) prominent peaks appear and we assign them accordingly:  
2817 cm<sup>-1</sup> (s-CH<sub>2</sub>), 2848 cm<sup>-1</sup> (s-CH<sub>3</sub>), 2895 and 2908 cm<sup>-1</sup>  
(both s-OCH<sub>2</sub>), 2960 cm<sup>-1</sup> (as-CH<sub>3</sub>), 2980 and 3022 cm<sup>-1</sup>  
(both as-OCH<sub>2</sub>).

We suggest that at ~1.0 V the ethoxy radical (or anion,  
CH<sub>3</sub>CH<sub>2</sub>O<sup>-</sup>) reacts with acidic surface Si sites (Si-H) and  
substitutes the proton with an ethoxy group to produce a Si-  
ethoxy bond (Si-OCH<sub>2</sub>CH<sub>3</sub>). It has been proposed that all  
linear carbonates decompose via a linear alkyl anion (in our  
case the ethoxy anion CH<sub>3</sub>CH<sub>2</sub>O<sup>-</sup> featured in Scheme 1).<sup>36</sup>

We assume that the ethoxy radical/anion is the most likely  
species to chemically react with the oxide layer of the Si anode  
surface. The other electrolyte component, usually cyclic ether  
(ethylene carbonate in this study), cannot form an ethoxy  
radical. Therefore, even if EC is reduced before DEC it is the  
reduction of DEC to ethoxy that is significant in the anode  
surface substitution reaction.

In order to acquire a spectrum of a Si-ethoxy, we produced a  
Si-ethoxy wafer and the obtained SFG-VS spectrum of this  
sample is presented in Figure 3. The procedure is similar to the  
one reported by Michalak et al.<sup>37,38</sup> and is discussed in the  
Supporting Information (SI). The major peaks that we  
observed were at the following frequencies, and we have  
assigned them accordingly:<sup>39</sup> 2875 cm<sup>-1</sup> (s-CH<sub>3</sub>), 2895 cm<sup>-1</sup>  
(s-OCH<sub>2</sub>), 2912 cm<sup>-1</sup> (Fermi), 2952 cm<sup>-1</sup> (as-CH<sub>3</sub>), and 2975  
and 3040 cm<sup>-1</sup> (both as-OCH<sub>2</sub>). Obviously, the presence (or  
absence) of these peaks tells us if indeed Si-ethoxy sites are  
present.

According to previous calculations by Wang et al.<sup>40</sup> we  
assume that EC does not react with the Si-H surface as its  
intermediate anions swiftly reduce to LiEDC. Furthermore, we  
postulate that even if there is such bond formation, the surface  
concentration will be below our detection limit (less than a 0.1

Scheme 1. Proposed Formation Pathways of Electrolyte Reduction Products<sup>4a</sup>

(a) Common to all DEC decomposition chemical pathways is the  $\text{CH}_3\text{CH}_2\text{O}^-$  anion formation. In accordance with our findings this anion replaces the hydrogen terminated Si with an ethoxy group. (b) A proposed mechanism to the reduction of EC to poly-EC by a Lewis acid ( $\text{PF}_5$ ).<sup>9</sup> (c) A suggested ring opening mechanism to form LiEDC.

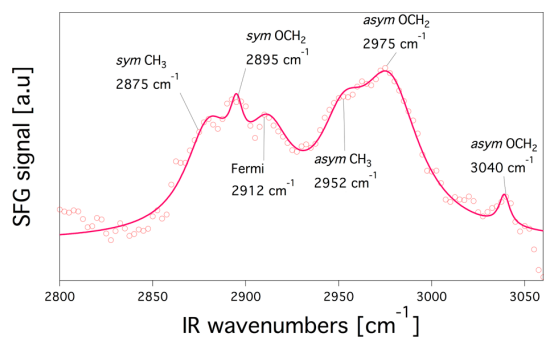


**Figure 3.** SFG profile of Si(100)- $\text{OC}_2\text{H}_5$ . The peaks frequencies and their bond assignments are noted in the figure. Experimental data is presented in dots, and fitting with a Lorentzian peak function is shown as a solid line.

monolayer) due to steric effects blocking neighboring sites.<sup>37,38</sup> To further exclude the reduction of EC near the Si anode surface in the presence of  $\text{LiPF}_6$  to form a Si compound, we have taken SFG spectra of 1.0 M  $\text{LiPF}_6$ :EC (diluted in *d*-THF to 3%, v/v) in contact with the Si(100)-H terminated wafer at two potential ranges ( $\sim 1.0$  V and  $\sim 0.5$  V).

In Figure 4, we present the SFG intensity (i.e., the SFG of CV divided by the OCP spectrum) of EC on Si(100)-hydrogen terminated after cyclic voltammetry at 1.1 V  $\leftrightarrow$  0.8 V (black) and 0.65 V  $\leftrightarrow$  0.35 V (red). The SFG intensity profile at  $\sim 1$  V has no detectable features as expected since EC reduction onset potential is at  $\sim 0.5$  V. Once we lowered the applied potential to about 0.5 V (red curve), new peaks appeared that we assigned to poly-EC and LiEDC. Nevertheless, at  $\sim 1$  V the absence of a peak at  $2895\text{ cm}^{-1}$  corresponding to the *s*- $\text{OCH}_2$  group stretch associated with the Si-ethoxy formation reveals that only the reduction of DEC leads to Si-ethoxy formation. For poly-EC we assign the peaks at  $2948$  and  $3000\text{ cm}^{-1}$ , and the peaks related to LiEDC are assigned at  $2890$ ,  $2965$ , and  $2980\text{ cm}^{-1}$ .<sup>29</sup>

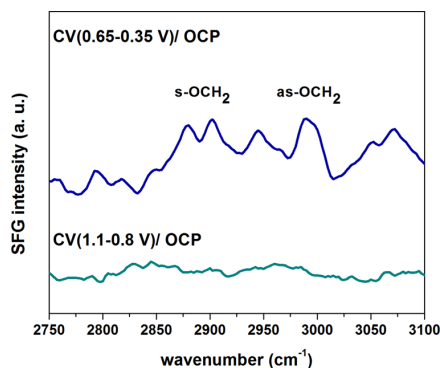


**Figure 4.** SFG intensity (i.e., divided by the OCP spectrum) of ethylene carbonate (EC) on Si(100)-hydrogen terminated after cyclic voltammetry at 1.1 V  $\leftrightarrow$  0.8 V (cyan) and 0.65 V  $\leftrightarrow$  0.35 V (blue).

In conclusion, by performing SFG-VS together with CV we have observed that the Si-hydrogen terminated layer has been changed to Si-ethoxy (Si- $\text{OCH}_2\text{CH}_3$ ) at a potential close to 1.0 V only when DEC is present. The role of each electrolyte component (EC and DEC) was investigated separately. This substitution reaction at  $\sim 1.0$  V did not take place when we changed the electrolyte to 1.0 M  $\text{LiPF}_6$  in EC or when the Si(100)- $\text{O}_x$  was used as the anode material. When we further reduced the potential to  $\sim 0.5$  V only poly-EC and LiEDC formation was observed. Further in situ spectroelectrochemical (SFG-VS and CV) experiments of EC at reduction potentials of  $\sim 1.0$  V and  $\sim 0.5$  V suggest that it has been possibly reduced to poly-EC, but no Si-ethoxy termination was detected. Future SFG-VS in the  $\text{C}=\text{O}$  carbonyl stretch range and CV experiments are planned.

## ASSOCIATED CONTENT

### Supporting Information

The Supporting Information is available free of charge on the ACS Publications website at DOI: 10.1021/jacs.5b10333.

Additional information about the SFG apparatus, spectroelectrochemical half-cell set up, and general chemical description (PDF)

## AUTHOR INFORMATION

### Corresponding Author

\*E-mail: Somorjai@Berkeley.edu.

### Author Contributions

<sup>§</sup>These authors contributed equally.

### Notes

The authors declare no competing financial interest.

## ACKNOWLEDGMENTS

This work was supported by the Assistant Secretary for Energy Efficiency and Renewable Energy, Office of Freedom CAR and Vehicle Technologies of the U.S. Department of Energy under Contract No. DE-AC02 OSCH1123. The SFG instrumentation was purchased with funding from the Director, Office of Basic Energy Sciences, Materials Science and Engineering Division of the U.S. Department of Energy. This work was also funded through a grant from Honda Research Institute. The authors also wish to thank E. Edri and N. Kornienko for their technical insights and support.

## 221 ■ REFERENCES

- 222 (1) Goodenough, J. B.; Park, K.-S. *J. Am. Chem. Soc.* **2013**, *135*, 1167.  
223 (2) Kraysberg, A.; Ein-Eli, Y. *Adv. Energy Mater.* **2012**, *2*, 922.  
224 (3) Obrovac, M. N.; Krause, L. J. *J. Electrochem. Soc.* **2007**, *154*, A103.  
225 (4) Liu, N.; Lu, Z.; Zhao, J.; McDowell, T. M.; Lee, H.-W.; Zhao, W.;  
226 Cui, Y. *Nat. Nanotechnol.* **2014**, *9*, 187.  
227 (5) Xu, K.; von Cresce, A. V. *J. Mater. Chem.* **2011**, *21*, 9849.  
228 (6) Peled, E. *J. Electrochem. Soc.* **1979**, *126*, 2047.  
229 (7) Peled, E.; Golodnitsky, D.; Ardel, G. *J. Electrochem. Soc.* **1997**,  
230 *144*, L208.  
231 (8) Ross, P. N. *Catal. Lett.* **2014**, *144*, 1370.  
232 (9) Shi, F.; Ross, P. N.; Zhao, H.; Liu, G.; Somorjai, G. A.;  
233 Komvopoulos, K. *J. Am. Chem. Soc.* **2015**, *137*, 3181.  
234 (10) Shi, F.; Zhao, H.; Liu, G.; Ross, P. N.; Somorjai, G. A.;  
235 Komvopoulos, K. *J. Phys. Chem. C* **2014**, *118*, 14732.  
236 (11) Zhao, J.; Lu, Z.; Wang, H.; Liu, W.; Lee, H.-W.; Yan, K.; Zhuo,  
237 D.; Lin, D.; Liu, N.; Cui, Y. *J. Am. Chem. Soc.* **2015**, *137*, 8372.  
238 (12) Philippe, B.; Dedryvère, R.; Allouche, J.; Lindgren, F.; Gorgoi,  
239 M.; Rensmo, H.; Gonbeau, D.; Edström, K. *Chem. Mater.* **2012**, *24*,  
240 1107–1115.  
241 (13) Schroder, K. W.; Dylla, A. G.; Harris, S. J.; Webb, L. J.;  
242 Stevenson, K. J. *ACS Appl. Mater. Interfaces* **2014**, *6*, 21510–21524.  
243 (14) Schroder, K.; Alvarado, J.; Yersak, T. A.; Li, J.; Dudney, N.;  
244 Webb, L. J.; Meng, Y. S.; Stevenson, K. J. *Chem. Mater.* **2015**, *27*,  
245 5531–5542.  
246 (15) Li, S. R.; Sinha, N. N.; Chen, C. H.; Xu, K.; Dahn, J. R. J.  
247 *Electrochem. Soc.* **2013**, *160*, A2014.  
248 (16) Nie, M.; Abraham, D. P.; Chen, Y.; Bose, A.; Lucht, B. L. *J. Phys.*  
249 *Chem. C* **2013**, *117*, 13403–13412.  
250 (17) Xu, C.; Lindgren, F.; Philippe, B.; Gorgoi, M.; Björefors, F.;  
251 Edström, K.; Gustafsson, T. *Chem. Mater.* **2015**, *27*, 2591–2599.  
252 (18) Shen, Y. R. *Nature* **1989**, *337*, 519.  
253 (19) Romero, C.; Baldelli, S. *J. Phys. Chem. B* **2006**, *110*, 11936.  
254 (20) Mukherjee, P.; Lagutchev, A.; Dlott, D. D. *J. Electrochem. Soc.*  
255 **2012**, *159*, A244.  
256 (21) Nicolau, B. G.; García-Rey, N.; Dryzhakov, B.; Dlott, D. D. *J.*  
257 *Phys. Chem. C* **2015**, *119*, 10227.  
258 (22) Liu, H.; Tong, Y.; Kuwata, N.; Osawa, M.; Kawamura, J.; Ye, S.  
259 *J. Phys. Chem. C* **2009**, *113*, 20531.  
260 (23) Yu, L.; Liu, H.; Wang, Y.; Kuwata, N.; Osawa, M.; Kawamura, J.;  
261 Ye, S. *Angew. Chem., Int. Ed.* **2013**, *52*, 5753.  
262 (24) Kolasinski, K. W. *Phys. Chem. Chem. Phys.* **2003**, *5*, 1270.  
263 (25) Schroder, K. W.; Celio, H.; Webb, L. J.; Stevenson, K. J. *J. Phys.*  
264 *Chem. C* **2012**, *116*, 19737.  
265 (26) Malyk, S.; Shalhout, F. Y.; O’Leary, L. E.; Lewis, N. S.;  
266 Benderskii, A. V. *J. Phys. Chem. C* **2013**, *117*, 935.  
267 (27) Ein-Eli, Y. *Electrochem. Solid-State Lett.* **1999**, *2*, 212.  
268 (28) Zhang, X.; Kostecki, R.; Richardson, T. J.; Pugh, J. K.; Ross, P.  
269 N. *J. Electrochem. Soc.* **2001**, *148*, A1341.  
270 (29) Haregewoin, A. M.; Leggesse, E. G.; Jiang, J.-C.; Wang, F.-M.;  
271 Hwang, B.-J.; Lin, S.-D. *Electrochim. Acta* **2014**, *136*, 274.  
272 (30) Bateman, J. E.; Eagling, R. D.; Horrocks, B. R.; Houlton, A. J.  
273 *Phys. Chem. B* **2000**, *104*, 5557.  
274 (31) Zhuang, G. V.; Xu, K.; Yang, H.; Jow, T. R.; Ross, P. N. *J. Phys.*  
275 *Chem. B* **2005**, *109*, 17567.  
276 (32) Xu, K.; Zhuang, G. V.; Allen, J. L.; Lee, U.; Zhang, S. S.; Ross, P.  
277 N.; Jow, T. R. *J. Phys. Chem. B* **2006**, *110*, 7708.  
278 (33) Chan, C. K.; Peng, H.; Liu, G.; McIlwrath, K.; Zhang, X. F.;  
279 Huggins, R. A.; Cui, Y. *Nat. Nanotechnol.* **2008**, *3*, 31.  
280 (34) Peng, K.; Jie, J.; Zhang, W.; Lee, S.-T. *Appl. Phys. Lett.* **2008**, *93*,  
281 033105.  
282 (35) Baranchugov, V.; Markevich, E.; Pollak, E.; Salitra, G.; Aurbach,  
283 D. *Electrochem. Commun.* **2007**, *9*, 796.  
284 (36) Haregewoin, A. M.; Shie, T.-D.; Lin, S.-D.; Hwang, B.-J. *ECS*  
285 *Trans.* **2013**, *S3*, 23.  
286 (37) Michalak, D. J.; Amy, S. R.; Aureau, D.; Dai, M.; Estève, A.;  
287 Chabal, Y. J. *Nat. Mater.* **2010**, *9*, 266.  
288 (38) Michalak, D. J.; Amy, S. R.; Aureau, D.; Estève, A.; Chabal, Y. J.  
289 *J. Phys. Chem. C* **2008**, *112*, 11907.  
(39) Gomes, J. F.; Bergamaski, K.; Pinto, M. F.S.; Miranda, P. B. J. *J.*  
*Catal.* **2013**, *302*, 67. 291  
(40) Wang, Y.; Nakamura, S.; Ue, M.; Balbuena, P. B. *J. Am. Chem.* *Soc.* **2001**, *123*, 11708–11718. 292  
293